

# Strangeness production in antiproton-nucleus collisions

A.B. Larionov · T. Gaitanos · U. Mosel

the date of receipt and acceptance should be inserted later

**Abstract** Antiproton annihilations on nuclei provide a very interesting way to study the behaviour of strange particles in the nuclear medium. In low energy  $\bar{p}$  annihilations, the hyperons are produced mostly by strangeness exchange mechanisms. Thus, hyperon production in  $\bar{p}A$  interactions is very sensitive to the properties of the antikaon-nucleon interaction in nuclear medium. Within the Giessen Boltzmann-Uehling-Uhlenbeck transport model (GiBUU), we analyse the experimental data on  $\Lambda$  and  $K_S^0$  production in  $\bar{p}A$  collisions at  $p_{\text{lab}} = 0.2 - 4$  GeV/c. A satisfactory overall agreement is reached, except for the  $K_S^0$  production in  $\bar{p}+^{20}\text{Ne}$  collisions at  $p_{\text{lab}} = 608$  MeV/c, where we obtain substantially larger  $K_S^0$  production rate. We also study the  $\Xi$  hyperon production, important in view of the forthcoming experiments at FAIR and J-PARC.

**Keywords**  $\bar{p}A$  collisions ·  $\Lambda$ ,  $K_S^0$  and  $\Xi$  production · BUU model

## 1 Introduction

About two decades ago several experiments have been done on strangeness production in  $\bar{p}$ -nucleus reactions. In the hydrogen bubble chamber experiment at BNL [1], the  $\Lambda$ -hyperon production in collisions  $\bar{p}(0 - 450\text{MeV/c}) + ^{12}\text{C}, ^{48}\text{Ti}, ^{181}\text{Ta}$  and  $^{208}\text{Pb}$  has been measured. At KEK [2,3], the hydrogen bubble chamber measurements have been performed for the  $K_S^0$ ,  $\Lambda$  and  $\bar{\Lambda}$  production from  $\bar{p}(4\text{ GeV/c}) + ^{181}\text{Ta}$ . Finally, at LEAR [4], the  $K_S^0$  and  $\Lambda$  rapidity yields from  $\bar{p}(607\text{ MeV/c}) + ^{20}\text{Ne}$  interactions have been studied using the streamer chamber filled with a natural  $^{20}\text{Ne}$  gas. Recently,  $K^\pm$  production in annihilation of stopped  $\bar{p}$ 's on p, d,  $^3\text{He}$  and  $^4\text{He}$  has been measured at LEAR [5] applying the magnetic spectrometer Obelix.

---

A.B. Larionov · T. Gaitanos · U. Mosel  
Institut fuer Theoretische Physik, Universitaet Giessen  
D-35392 Giessen, Germany  
E-mail: Alexei.Larionov@theo.physik.uni-giessen.de

A.B. Larionov  
Russian Research Center “Kurchatov Institute”, 123182 Moscow, Russia

These experiments revealed some interesting features which still remain to be explained by theory:

- Large ratio of the particle yields  $\Lambda/K_S^0 = 2 - 3$  both for light ( $^{20}\text{Ne}$ ) and heavy ( $^{181}\text{Ta}$ ) targets.
- $\Lambda$  rapidity spectrum peaked close to the target rapidity even for energetic collisions  $\bar{p}(4 \text{ GeV}/c) + ^{181}\text{Ta}$ .
- Enhanced strangeness production for  $\bar{p}$  annihilations at rest involving more than one nucleon (baryon number of annihilating system  $B > 0$ ).

In order to describe the yields of strange particles and, in particular, the large  $\Lambda/K_S^0$  ratio in  $\bar{p} + ^{181}\text{Ta}$  interactions at 4 GeV/c, Rafelski [6] assumed an annihilation fireball in the state of a supercooled quark-gluon plasma (QGP) propagating through the target nucleus and absorbing nucleons. Eventually, this fireball reaches a high baryon number,  $B \simeq 10$ , and then hadronizes producing the excess of strange particles. Such an exotic scenario has been questioned in the following-up theoretical work by Cugnon et al. [7], where the intranuclear cascade (INC) calculations of the strangeness production in  $\bar{p}$ -nucleus interactions have been performed.

In this talk, we present the results of our transport-theoretical analysis of experimental data on strangeness production from  $\bar{p}$ -nucleus interactions in-flight. We also make predictions on the  $\Xi$ -hyperon ( $S = -2$ ) and  $\Lambda$ -hypernuclear production. Section 2 contains a brief description of the GiBUU model applied in our calculations. In Section 3, we present the numerical results and discuss them. The summary is given in Section 4.

## 2 Model

The GiBUU transport model [8] solves the coupled system of relativistic kinetic equations for the different sorts of hadrons:

$$(p_0^*)^{-1} [p_\mu^* \partial_x^\mu + (p_\mu^* F_i^{\nu\mu} + m_i^* (\partial_x^\nu m_i^*)) \partial_\nu^{p^*}] f_i(x, \mathbf{p}^*) = I_i[\{f\}] , \quad (1)$$

where  $f_i(x, \mathbf{p}^*)$  with  $x \equiv (t, \mathbf{r})$  denotes the distribution function of the particles of sort  $i$  ( $i = N, \bar{N}, \Delta, \bar{\Delta}, Y, \bar{Y}, \Xi, \bar{\Xi}, \pi, \eta, \omega, \rho, K, \bar{K}, \dots$  taking into account isospin projections) in the six-dimensional phase space  $(\mathbf{r}, \mathbf{p}^*)$ . If the r.h.s. of Eq. (1), i.e. the collision term  $I_i[\{f\}]$ , would be zero, then Eq. (1) would be a classical Vlasov equation describing the propagation of the particles in the mean field potentials of a nuclear and electromagnetic nature.

The relativistic form of Eq. (1) needs to explain some specific quantities:  $p^{*\mu} = p^\mu - V_i^\mu$  is the kinetic four-momentum,  $F_i^{\mu\nu} \equiv \partial^\mu V_i^\nu - \partial^\nu V_i^\mu$  is the field tensor, and  $m_i^* = m_i + S_i$  is the effective mass. The particles are assumed to be on their in-medium mass shells,  $p_\mu^* p^{*\mu} = m_i^{*2}$ . The scalar and vector fields are expressed, respectively, as  $S_i = g_{\sigma i} \sigma$  and  $V_i^\mu = g_{\omega i} \omega^\mu + g_{\rho i} \tau^3 \rho^{3\mu} + q_i A^\mu$ . Here,  $\sigma$  ( $I = 0, J = 0$ ),  $\omega^\mu$  ( $I = 0, J = 1$ ) and  $\rho^\mu$  ( $I = 1, J = 1$ ) are the mean mesonic fields and  $A^\mu = (A^0, \mathbf{0})$  is the Coulomb field.

The mean mesonic and Coulomb fields are calculated, respectively, from the static Klein-Gordon-like and Poisson equations with the source terms provided by the space- and time-dependent particle densities and currents. The meson-nucleon coupling constants and the self-interaction parameters of the  $\sigma$ -field are

adopted from the NL3 version of the non-linear Walecka model [9]. The coupling constants of the other baryons with mean mesonic fields are obtained from the corresponding meson-nucleon coupling constants by simple rescaling taking into account the light-quark contents, and, for antibaryons, the G-parity symmetry and phenomenological depth of the antiproton optical potential ( $\text{Re}(V_{\text{opt}}) \simeq -150$  MeV in the nuclear center). This leads, e.g., to a  $\Lambda(\bar{\Lambda})$  potential of  $\simeq -40(-450)$  MeV and  $K(\bar{K})$  potential of  $\simeq -20(-220)$  MeV (see refs. [10,11,12] for further details of the mean fields).

The collision integral in the r.h.s. of Eq. (1) describes the antibaryon-baryon annihilation, elastic and inelastic hadron-hadron scattering processes, and resonance decays. It includes the elementary hadron-hadron cross sections and resonance widths as parameters. The elementary cross sections are obtained by phenomenological fits to experimental data or given by theoretical calculations.

The following *antibaryon-baryon* reaction channels are included:  $\bar{B}B \rightarrow$  mesons simulated by statistical annihilation model [13],  $\bar{B}B \rightarrow \bar{B}B$  (elastic and charge exchange),  $\bar{N}N \leftrightarrow \bar{N}\Delta(\bar{\Delta}N)$ ,  $\bar{N}N \rightarrow \bar{\Lambda}\Lambda$ ,  $\bar{N}N(\bar{N}\Delta, \bar{\Delta}N) \rightarrow \bar{\Lambda}\Sigma(\bar{\Sigma}\Lambda)$ ,  $\bar{N}N(\bar{N}\Delta, \bar{\Delta}N) \rightarrow \bar{\Xi}\Xi$ . For invariant energies  $\sqrt{s} > 2.4$  GeV ( $p_{\text{lab}} > 1.9$  GeV/c for  $\bar{N}N$ ), the inelastic production in antibaryon-baryon collisions,  $\bar{B}_1 B_2 \rightarrow \bar{B}_3 B_4 + \text{mesons}$ , is simulated with the help of the FRITIOF model.

The *baryon-baryon* reactions implemented in the model are:  $BB \rightarrow BB$  (elastic and charge exchange),  $NN \leftrightarrow NN\pi$ ,  $NN \leftrightarrow \Delta\Delta$ ,  $NN \leftrightarrow NR$ , where  $R$  denotes any nonstrange baryonic resonance,  $N(\Delta, N^*)N(\Delta, N^*) \rightarrow N(\Delta)YK$ ,  $YN \rightarrow YN$ ,  $\Xi N \rightarrow \Lambda\Lambda$ ,  $\Xi N \rightarrow \Lambda\Sigma$ ,  $\Xi N \rightarrow \Xi N$ . For  $\sqrt{s} > 2.4$  GeV, the inelastic production in baryon-baryon collisions,  $B_1 B_2 \rightarrow B_3 B_4 + \text{mesons}$ , is simulated by using the PYTHIA model.

The *meson-baryon* collisions taken into account in the model are:  $\pi N \leftrightarrow R$ ,  $\pi N \rightarrow K\bar{K}N$ ,  $\pi(\eta, \rho, \omega)N \rightarrow YK$ ,  $\bar{K}N \leftrightarrow Y^*$ ,  $\bar{K}N \rightarrow \bar{K}N$ ,  $\bar{K}N \leftrightarrow Y\pi$ ,  $\bar{K}N \leftrightarrow Y^*\pi$ ,  $\bar{K}N \rightarrow \Xi K$ . For  $\sqrt{s} > 2.2$  GeV, the meson-baryon collisions are simulated by applying the PYTHIA model.

The GiBUU model also includes the strangeness production/absorption channels in meson-meson collisions:  $MM \leftrightarrow \bar{K}(\bar{K}^*)K(K^*)$ , where  $M$  denotes any nonstrange meson ( $M = \pi, \eta, \eta', \sigma, \rho, \omega, \dots$ ). Further details on the elementary cross sections included in the model can be found on the GiBUU web-site [8] and in the review article [14].

### 3 Results

We start with the low beam momenta and consider the annihilations of  $\bar{p}$  at 225 MeV/c on several target nuclei. Figure 1 shows the probability of the  $\Lambda$  production per  $\bar{p}$  annihilation event on a nucleus as a function of the nucleus mass number. We have separated the  $\Lambda$  hyperons emitted to free space from those bound in the nuclear remnant at the end of time evolution ( $\simeq 200$  fm/c starting from  $\bar{p}$  at the longitudinal distance of nuclear radius + 5 fm from the nuclear centre). Our results on free  $\Lambda$ 's agree quite well with experiment. The probability of the bound  $\Lambda$ - ( $\Lambda\Lambda$ -) nuclear system production, as expected, grows with the target mass number reaching  $\simeq 3\%$  (0.01%) for the lead target.

In Fig. 2, we present the rapidity spectra of  $(\Lambda + \Sigma^0)$  and  $K_S^0$  for  $\bar{p}$  annihilations on  $^{20}\text{Ne}$  at 607 MeV/c. Since the  $\Sigma^0 \rightarrow \Lambda\gamma$  decay is not taken into account

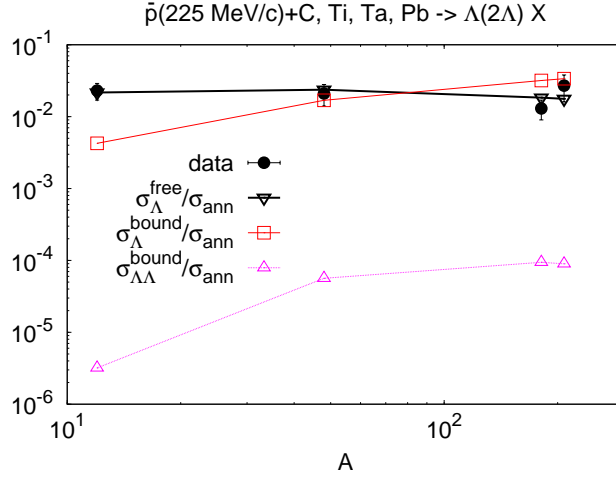
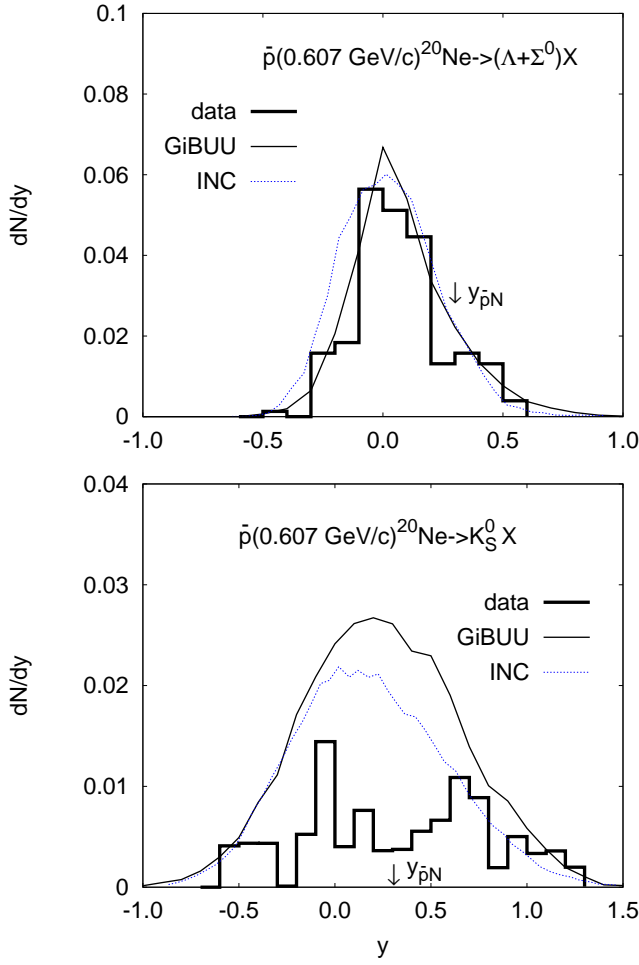


**Fig. 1** The cross sections of the free  $\Lambda$  production, bound  $\Lambda$  production, and two bound  $\Lambda$ 's production for  $\bar{p}(225 \text{ MeV/c}) + {}^{12}\text{C}$ ,  ${}^{48}\text{Ti}$ ,  ${}^{181}\text{Ta}$  and  ${}^{208}\text{Pb}$ . The cross sections are normalized on the annihilation cross sections of  $\bar{p}$  on the corresponding nuclei. The data for free  $\Lambda$ 's [1] are for the beam momentum range 0-450 MeV/c.

in GiBUU, we have summed up both  $\Lambda$  and  $\Sigma^0$  spectra in order to compare with experimental data. The data on  $\Lambda$ -rapidity yields are described quite well by GiBUU. By studying the  $Y(Y^*)$  production rate more in-detail, we have found that  $\sim 80\%$  of this rate is due to the strangeness exchange reactions of the type  $\bar{K}N \rightarrow Y\pi$ .

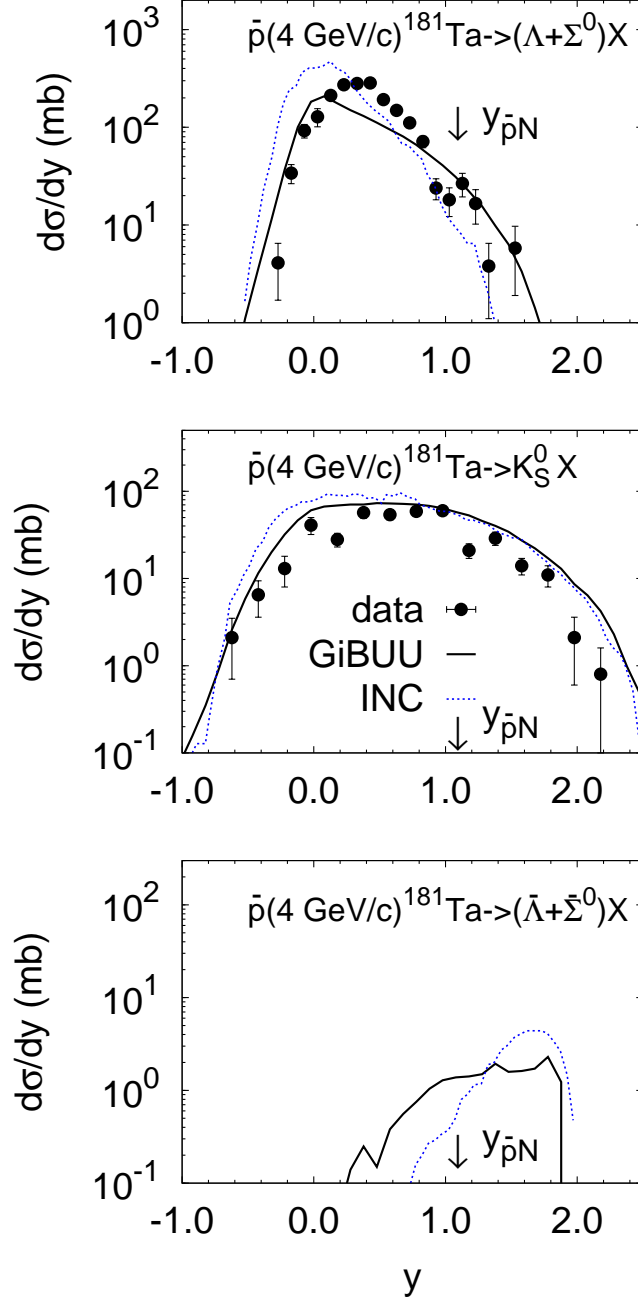
The calculated  $K_S^0$  yield,  $N_{K_S^0} = (N_{K^0} + N_{\bar{K}^0})/2$ , is considerably higher than experiment, as one can see from Fig. 2. The INC calculations [7] are also in a rather good agreement with  $\Lambda$  rapidity spectrum, but overpredict the  $K_S^0$  production.

Fig. 3 presents the  $(\Lambda + \Sigma^0)$ ,  $K_S^0$  and  $(\bar{\Lambda} + \bar{\Sigma}^0)$  rapidity spectra from  $\bar{p} + {}^{181}\text{Ta}$  collisions at 4 GeV/c. The GiBUU model reproduces the tails of the  $y$ -distribution of  $\Lambda$ 's fairly well, but underestimates the data at the peak position,  $y \simeq 0.3$ . On the other hand, the INC model overestimates the data around the target rapidity,  $y = 0$ . Both models produce the peak position of the  $\Lambda$  rapidity spectrum at  $y \simeq 0$ . The theoretical rapidity spectra of  $K_S^0$  agree with data reasonably well, except for target rapidities, where some excess of  $K_S^0$  is still visible. By inspecting the  $Y(Y^*)$  production rate we again found that  $\sim 70 - 80\%$  of this rate is due to the strangeness exchange processes  $\bar{K}(\bar{K}^*)B \rightarrow YX$ ,  $\bar{K}B \rightarrow Y^*$ , and  $\bar{K}B \rightarrow Y^*\pi$ , while the total contribution of the  $\bar{B}B$  collision channels — including the direct  $\bar{N}N$  channel — is on the level of a few percent only. The difference between the  $(\bar{\Lambda} + \bar{\Sigma}^0)$  rapidity spectra produced by GiBUU and INC is mostly due to somewhat different angular distributions for the  $\bar{N}N \rightarrow \bar{Y}Y$  processes and due to different  $\bar{Y}N$  annihilation cross sections used in the both models. We also note that the INC model does not contain mean field potentials, while our calculations include strongly attractive antihyperon potentials.



**Fig. 2** The rapidity distributions of the  $(\Lambda + \Sigma^0)$  hyperons and  $K_S^0$  from  $\bar{p}(607 \text{ MeV}/c) + {}^{20}\text{Ne}$  annihilations. The distributions are normalized so that their integrals over  $y$  give the number of particles per annihilation event. The INC calculations from [7] are also shown. The data (histograms) are from ref. [4]. Vertical arrows indicate the rapidity of a  $\bar{p}$ -nucleon center-of-mass (c.m.) system.

Let us, finally, discuss the predictions of the GiBUU model for the  $S = -2$  hyperon production in  $\bar{p} + {}^{197}\text{Au}$  collisions at 3 GeV/c. We have found that the predominant channel of  $\Xi$ -hyperon production is the collisions of the strange mesons  $\bar{K}$ ,  $\bar{K}^*$ ,  $K$  and  $K^*$  with baryons which are responsible for  $\sim 35\%$  of the total  $\Xi$  yield. Almost of the same importance are the  $\Xi^* \rightarrow \Xi\pi$  decays ( $\sim 26\%$ ), and strange meson-hyperon collisions ( $\sim 17\%$ ). The direct channel  $\bar{N}N \rightarrow \bar{\Xi}\Xi$  is responsible only for a quite small fraction of produced  $\Xi$ 's ( $\sim 5\%$ ).



**Fig. 3** The  $(\Lambda + \Sigma^0)$ ,  $K_S^0$  and  $(\bar{\Lambda} + \bar{\Sigma}^0)$  rapidity distributions for the collisions  $\bar{p}(4 \text{ GeV}/c)^{181}\text{Ta}$ . The INC calculations are taken from [7]. The data are from [3].

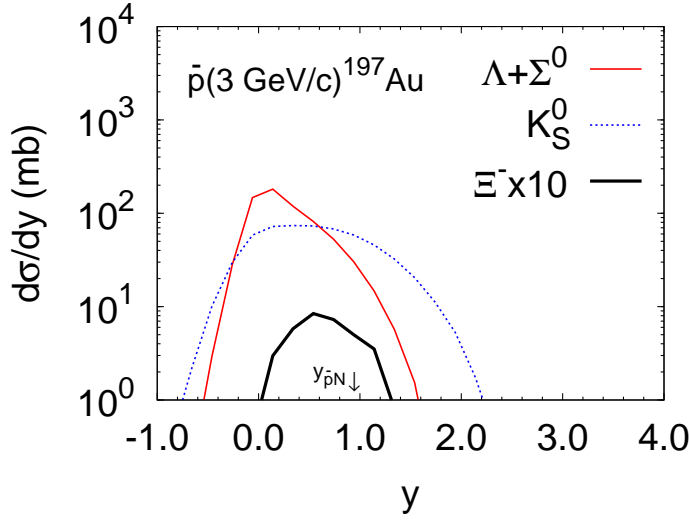


**Fig. 4** Rapidity distributions of  $(\Lambda + \Sigma^0)$ ,  $\Xi^-$  and  $K_S^0$  from  $\bar{p}$  interactions with  $^{197}\text{Au}$  at 3 GeV/c. The spectrum of  $\Xi^-$  hyperons is multiplied by a factor of 10.

Fig. 4 shows the rapidity spectra of  $\Xi^-$ ,  $(\Lambda + \Sigma^0)$  and  $K_S^0$  for the  $\bar{p}(3 \text{ GeV/c}) + ^{197}\text{Au}$  collisions. The spectra of the  $(\Lambda + \Sigma^0)$  hyperons are peaked close to  $y = 0$ . The  $K_S^0$  spectra have also a maximum at  $y \simeq 0$  spread towards forward rapidities. This behaviour has been interpreted in [6] as a signature of strangeness production from a QGP fireball. In this picture, the rapidity spectra of all strange particles emitted from the fireball should have their maxima at the c.m. rapidity of the fireball. However, the spectrum of  $\Xi^-$  hyperons produced by GiBUU calculations is shifted to the forward rapidities and peaked at  $y \simeq 0.6$ . The difference between the  $(\Lambda + \Sigma^0)$  and  $\Xi^-$  rapidity spectra can be understood in our pure hadronic transport calculations as the consequence of different thresholds for  $Y$  and  $\Xi$  production in antikaon-nucleon collisions. Indeed, the  $S = -1$  hyperons are mostly produced in exothermic reactions, like  $\bar{K}N \rightarrow Y\pi$ , with slow initial  $\bar{K}$ . As a result, the produced hyperon  $Y$  is also slow and its momentum is isotropically distributed in the laboratory frame. However, the double strangeness exchange process,  $\bar{K}N \rightarrow \Xi K$ , mainly responsible for  $\Xi$  production, is endothermic ( $p_{\text{lab}}^{\text{thr}} = 1.05 \text{ GeV/c}$  —  $\bar{K}$  beam momentum at threshold,  $y_{\text{c.m.}}^{\text{thr}} = 0.55$  — c.m. rapidity at threshold) and requires a fast incoming  $\bar{K}$ . Such antikaons are mostly emitted in the forward direction in the laboratory frame. Thus, the outgoing  $\Xi^-$  moves also forward due to the c.m. motion of the  $\bar{K}N$  system.

## 4 Summary

We have performed microscopic transport calculations of strangeness production in antiproton-nucleus collisions at  $p_{\text{lab}} = 0.2 - 4$  GeV/c on the basis of the GiBUU model. The main results can be summarized as follows:

- The experimental data on  $\Lambda$ -yields are reasonably well described. However, there are some deviations in detailed shape of  $\Lambda$ -rapidity spectrum at 4 GeV/c. The  $K_S^0$ -yields are overestimated. The yield ratios for  $\bar{p}+^{20}\text{Ne}$  at 608 MeV/c are:  $\Lambda/K_S^0 = 1.0$  (GiBUU),  $\Lambda/K_S^0 = 1.4$  (INC),  $\Lambda/K_S^0 = 2.3 \pm 0.7$  (exp.). This indicates missing antikaon absorption by  $\bar{K}N \rightarrow Y\pi$  in transport calculations.
- The peak positions of the  $(\Lambda + \Sigma^0)$ - and  $\Xi$ -hyperon rapidity spectra strongly differ. In future experiments at FAIR and J-PARC, this can be tested in order to support or exclude the possible exotic mechanism of strangeness production via a QGP fireball.
- $\Lambda$ - and  $\Lambda\Lambda$ -hypernuclei production is possible on the primary target at low  $\bar{p}$ -beam momenta.

**Acknowledgements** The support by the Frankfurt Center for Scientific Computing is gratefully acknowledged. This work was financially supported by the Bundesministerium für Bildung und Forschung, by the Helmholtz International Center for FAIR within the framework of the LOEWE program, and by the Grant NSH-7235.2010.2 (Russia).

## References

1. G.T. Condo, T. Handler, H.O. Cohn, Phys. Rev. **C29**, 1531 (1984)
2. K. Miyano, et al., Phys. Rev. Lett. **53**, 1725 (1984)
3. K. Miyano, et al., Phys. Rev. **C38**, 2788 (1988)
4. F. Balestra, et al., Phys. Lett. **B194**, 192 (1987)
5. G. Bendiscioli, T. Bressani, L. Lavezzi, A. Panzarasa, P. Salvini, Nucl. Phys. A **815**, 67 (2009)
6. J. Rafelski, Phys. Lett. **B207**, 371 (1988)
7. J. Cugnon, P. Deney, J. Vandermeulen, Phys. Rev. **C41**, 1701 (1990)
8. <http://gibuu.physik.uni-giessen.de/GiBUU>
9. Lalazissis, G. A. and König, J. and Ring, P., Phys. Rev. **C55**, 540 (1997)
10. I.N. Mishustin, L.M. Satarov, T.J. Bürvenich, H. Stöcker, W. Greiner, Phys. Rev. **C71**, 035201 (2005)
11. A.B. Larionov, I.A. Pshenichnov, I.N. Mishustin, W. Greiner, Phys. Rev. **C80**, 021601 (2009)
12. T. Gaitanos, A.B. Larionov, H. Lenske, U. Mosel, Phys. Rev. **C81**, 054316 (2010)
13. I.A. Pshenichnov, Statistical description of the reactions of multiple meson production on nuclei (in Russian). Ph.D. thesis, INR Moscow (1998)
14. O. Buss, T. Gaitanos, K. Gallmeister, H. van Hees, M. Kaskulov, O. Lalakulich, A. Larionov, T. Leitner, J. Weil, U. Mosel, (2011). E-print arXiv:1106.1344, accepted in Phys. Rept.